

No.5

Direct Numerical Simulation By LBM and Analyses of Two-dimensional Isotropic Turbulence

Ao-kui Xiong

Department of Machine Intelligence and Systems Engineering
Graduate School of Engineering, Tohoku University
Aoba-yama 01, Aoba-ku, Sendai 980-8579, JAPAN

Direct numerical simulations of the forced two-dimensional turbulence are performed by lattice Boltzmann method with high resolutions. It is confirmed that the lattice Boltzmann method is an alternative approach to simulate multi-scales flows efficiently before instability takes place. The instability can occur even after millions time-steps of iteration. Based on the database of the DNS, the behaviors of energy and enstrophy flux and the features of SGS Lamb vector in context of large eddy simulation are discussed. The most important observation is that the transverse component of the SGS Lamb vector, which plays a key role in the dynamics, only dominates in the regions of curved sheet-like structures.

Key Words: *Direct numerical simulation, Lattice Boltzmann method, Two-dimensional turbulence*

1. Introduction

In the past a few more than a decade, the lattice Boltzmann method (LBM), originated firstly from lattice-gas cellular automaton (LGA), has greatly developed into an alternative and promising numerical scheme for simulating fluid flows and modeling physics in fluids.¹⁾ Contrasting with the conventional CFD method, LBM is not a technique of numerical scheme or algorithm but a physical model of fluid flows with some advantages. Remarkable one of those is that it is a high efficient parallel method to simulate turbulent flows with multi-scales.

One class of physical systems exhibiting apparent two-dimensional turbulent behaviors is the large-scale motion of the Earth's air and ocean masses that occurs at a state close to geostrophic and hydrostatic balance.²⁾ Another motivation of the studies on two-dimensional turbulence is that it provides a beautiful example of dynamic system. In the past thirty years, a number of theoretical, numerical and experimental studies have been devoted to the understanding of this branch of fluid mechanics. But still, many fundamental questions remain open.³⁾ In this paper, direct numerical simulations of the forced two-dimensional turbulence are conducted by lattice Boltzmann method with high resolutions. Based on the database obtained by DNS, the behaviors of energy and enstrophy flux and the features of SGS Lamb vector in context of large eddy simulation are discussed. The emphases are on the interaction between large-scale and small-scale in two-dimensional turbulence that has been paid less attention.

2. Lattice Boltzmann Method

Instead of macro variables such as velocity and pressure, lattice Boltzmann method deals with mesoscopic quantities called distribution functions, which describe the fraction of masses of fluid bulk moving with a certain speed and are governed by, in a standard form

$$f_{\alpha}(\mathbf{x} + \mathbf{c}_{\alpha}\Delta t, t + \Delta t) = f_{\alpha}(\mathbf{x}, t) - \frac{f_{\alpha}(\mathbf{x}, t) - f_{\alpha}^{eq}(\rho, \mathbf{u})}{\tau}$$

In which, τ is relaxation time. f_{α} is equilibrium distribution function, related only to macroscopic states of the system

$$f_{\alpha}^{eq}(\rho, \mathbf{u}) = \rho w_{\alpha} [1 + 3c_{\alpha}u_i + \frac{9}{2}(c_{\alpha}u_i)^2 - \frac{3}{2}u_iu_i]$$

For two-dimensional flows, w_{α} takes

$$w_0 = \frac{4}{9}, w_{\alpha} = \frac{1}{9} (\alpha = 1, 3, 5, 7), w_{\alpha} = \frac{1}{36} (\alpha = 2, 4, 6, 8)$$

The formulas of the equilibrium distribution function are derived under some fundamental conservative laws about collision such as mass and momentum conservations.

Finally, the macro density and velocity of fluid flows are recovered by

$$\rho(\mathbf{x}, t) = \sum_{\alpha} f_{\alpha}(\mathbf{x}, t)$$

$$\mathbf{u}(\mathbf{x}, t) = \frac{\sum_{\alpha} \mathbf{c}_{\alpha} f_{\alpha}(\mathbf{x}, t)}{\rho(\mathbf{x}, t)}$$

It can be demonstrated that these density and velocity distributions satisfy the Navier-Stokes equations of viscous incompressible flow in second order of accuracy. Moreover, the pressure of the flow fields can be recovered by a isothermal state equation and the viscosity of the fluid is restored as

$$\mu = \Delta t (\tau - 0.5) \rho c_s^2$$

The most challenge in DNS using LBM is the instability occurring usually when Reynolds number is high enough. This instability can take place either at first several stages of simulation or even after millions time steps of iteration just as what happened in our case.

3. Simulation and analysis

Two-dimensional turbulences are different very much from the three-dimensional turbulent flows in the sense that there exist two opposite cascades in two-dimensional turbulence: energy (or inverse) cascade and enstrophy (or direct) cascade. Our simulations began from still initial condition with 512^2 resolution. The flow was driven by external force only with three lowest wavenumber modes in Fourier space. This process of evolution is of pure direct cascade that means both of energy and enstrophy transfer from large scales to small scales before stationary state is reached, as shown in Fig.1. To get database of higher resolution, we continued simulation with 1024^2 and 2048^2 resolutions, by rescaling double periodic domains of flow field with lower resolution as the latter's initial condition for time-saving. In these cases, the spectra of small scales underwent decaying, which usually implies inverse cascade. The spectral evolution of 2048^2 resolution was shown in Fig.2. Fig.3 shows the energy and enstrophy flux through fields of different scales at very late stage of time development. Positive value means flux from large-scale to small-scale for enstrophy but from small-scale to large-scale for energy flux. One can see here that inverse energy cascade and direct enstrophy cascade co-exist simultaneously. Note that the energy fluxes are very small especially for the smallest scales. This is consistent with the physical phenomena, saying that the like sign vortices will merge and the smallest eddies are easily and quickly merged into larger vortices. Fig.4 shows a typical vorticity distribution of forced two-dimensional turbulence. Sheet-like structures are characteristic pattern of the direct cascade.

The interaction between scales is the key point of understanding turbulent flows. In the engineering turbulence computations, models have to be used. Success of these computations heavily depends on whether or not the models mimic as closely as possible the interplaying behaviors. By filtering database of DNS, the instantaneous turbulent field was decomposed into scales- resolved and subgrid-scales parts in the context of large eddy simulation. Fig.5 shows a example of decomposed signal and vorticity field respectively. The distinct observation from the latter figure is that the large-scale structures that usually depend on initial condition and external force remained its marks in small-scale field.

For energy transfer between the resolved and subgrid fields, the inner product of additional stress with mean strain rate is broadly used like following

$$\begin{aligned} \frac{D}{Dt} \left(\frac{1}{2} \overline{u_i u_i} \right) = & - \frac{\partial}{\partial x_i} \left(\frac{\overline{u_i p}}{\rho} + \overline{u_i \tau_{ij}^R} \right) + \nu \frac{\partial^2}{\partial x_j \partial x_j} \left(\frac{1}{2} \overline{u_i u_i} \right) \\ & - \nu \frac{\partial \overline{u_i}}{\partial x_j} \frac{\partial \overline{u_i}}{\partial x_j} + \tau_{ij}^R \overline{S_{ij}} \end{aligned}$$

But there is no rigorous demonstration showing this is solely correct choice. Other candidates of transfer effects

come from the Helmholtz-Hodge decomposition of the nonlinear term in governing equations

$$\begin{aligned} \frac{D}{Dt} \left(\frac{1}{2} \overline{u_i u_i} \right) = & - \frac{\partial}{\partial x_i} \left(\frac{\overline{u_i p}}{\rho} \right) + \nu \frac{\partial^2}{\partial x_j \partial x_j} \left(\frac{1}{2} \overline{u_i u_i} \right) \\ & - \nu \frac{\partial \overline{u_i}}{\partial x_j} \frac{\partial \overline{u_i}}{\partial x_j} + \overline{u_i L_i} \end{aligned}$$

here

$$\begin{aligned} \overline{L_i u_i} = & - \overline{\boldsymbol{\omega} \times \mathbf{u} \bullet \mathbf{u}} \\ = & \nabla \bullet (\overline{\mathbf{u} \boldsymbol{\varphi}}) + (\nabla \times \boldsymbol{\Psi}) \bullet \overline{\mathbf{u}} \\ = & \nabla \bullet (\overline{\mathbf{u} \boldsymbol{\varphi}} + \boldsymbol{\Psi} \times \overline{\mathbf{u}}) + \boldsymbol{\Psi} \bullet \overline{\boldsymbol{\omega}} \end{aligned}$$

therefore, there are four possible forms of energy transfer

$$\tau_{ij}^R \overline{S_{ij}}, \quad \mathbf{L} \bullet \overline{\mathbf{u}}, \quad (\nabla \times \boldsymbol{\Psi}) \bullet \overline{\mathbf{u}}, \quad \boldsymbol{\Psi} \bullet \overline{\boldsymbol{\omega}}$$

Fig.6 shows the distributions of the four forms of energy transfer. The most interesting observation is for the final form of the four energy transfer terms to be smoother and then to be more adequate to be modeled in engineering computation. It is this quantity that was employed by Perot in his new RANS model as energy budget.⁴⁾ It also should be noticed that the enstrophy transfer has only sole form directly related to the transverse component (or, in other name, the vector potential part) of the Helmholtz-Hodge decomposition. All of these strongly suggest that the transverse component plays an important role in the interaction of resolved scales and subgrid scales. But more interestingly, the transverse component is only in the region of curved sheet-like structures to be over longitudinal component in amplitude just as shown in Fig.7, where the valuable is defined as

$$\Theta = (\nabla \times \boldsymbol{\Psi}) \bullet \mathbf{L} / L^2$$

4. Concluding remarks

Contrasting with the conventional CFD method, LBM is not a technique of numerical scheme or algorithm but a physical model of fluid flows with some advantages. Remarkable one of those is that it is a high efficient parallel method to simulate turbulent flows with multi-scales. The main challenge in this area is about instability when high Reynolds number's flows are to be simulated. Instability may take place even after millions time-steps of iteration. This strongly implies that it is quite different from that usually met in simulations of fluid flows and then distinct explanation needs to be given.

Generations of sheet-like structures and/or mergence/aggregation among vortices with like sign are fundamental phenomena of two-dimensional turbulence. The former corresponds to enstrophy (or direct) cascade, while the latter is regarded as energy (or inverse) cascade. For pure enstrophy (energy) cascades the energy (enstrophy), accompanying enstrophy (energy), are transferred from larger (smaller) scales to smaller (larger) ones. For co-existing cases, behaviors seem complicated. In our case, directly cascading of enstrophy and inversely cascading of energy are observed simultaneously. But the latter is very weak because it is after a long time of

evolution and therefore the energy from the small-scales is exhausted. The effects of large-scale structures generally dependent on initial condition and external circumstance remain in small-scale turbulence. The vector potential of SGS Lamb vector plays key role in the interactions of the resolved and the residual fields and much more smooth. Therefore, it should be more appropriate to be modeled in the context of large eddy simulation. Though its influence is great, the proportion of its curl (i.e. the transversal part of the SGS Lamb vector) is less than the longitudinal part, except where sheet-like structures are more heavily curved.

References

- 1) Chen, S. and Doolen, G.D., Annul. Rev. Fluid Mech., 30, 329-364(1998)
- 2) Vorobieff, P., Rivera, M., and Ecke, R.E., Phys. Fluids, 11, 2167-2177(1999)
- 3) Tabeling, P., Phys. Rep., 362, 1-62(2002)
- 4) Perot, B., Phys. Fluids, 11, 2645-2655(1999)

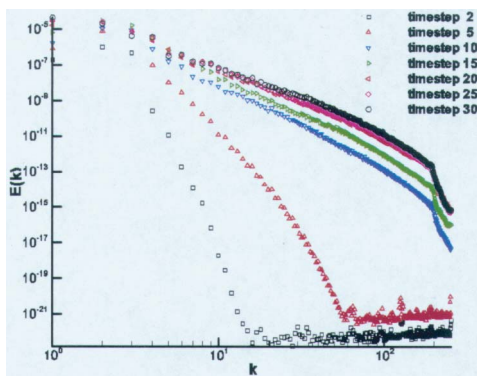


Figure 1. Time development of spectra for the 512² run.

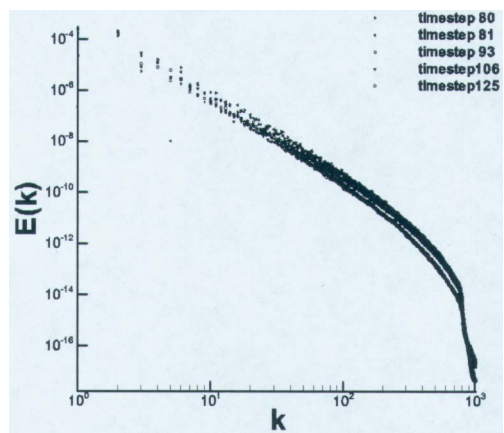


Figure 2. Time development of spectra for the 2048² run.

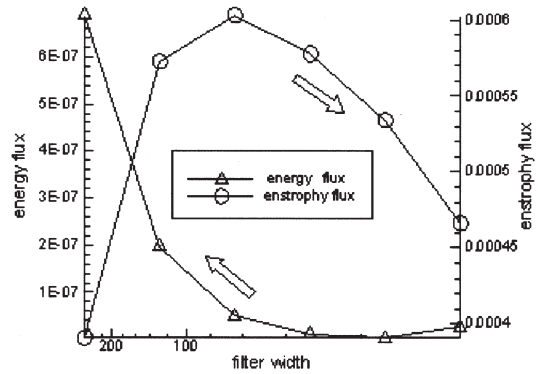


Figure 3. Spatial average energy and enstrophy flux through different scales.

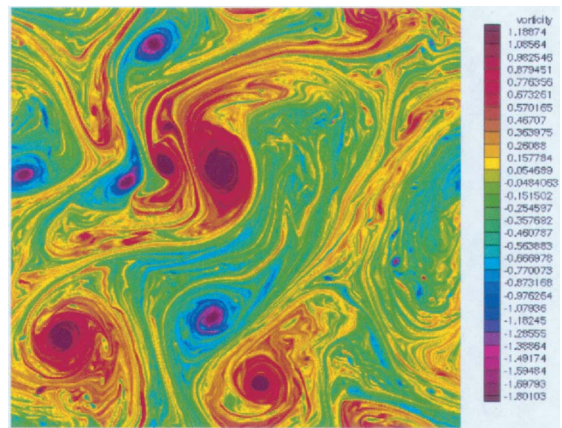


Figure 4. Distribution of vorticity.

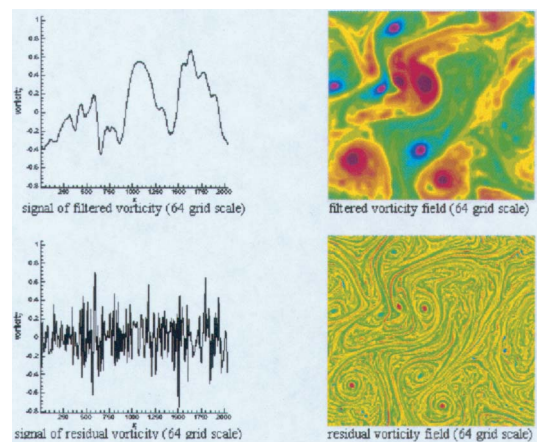


Figure 5. Signals (left) and flood contours (right) of resolved and subgrid vorticity distribution.

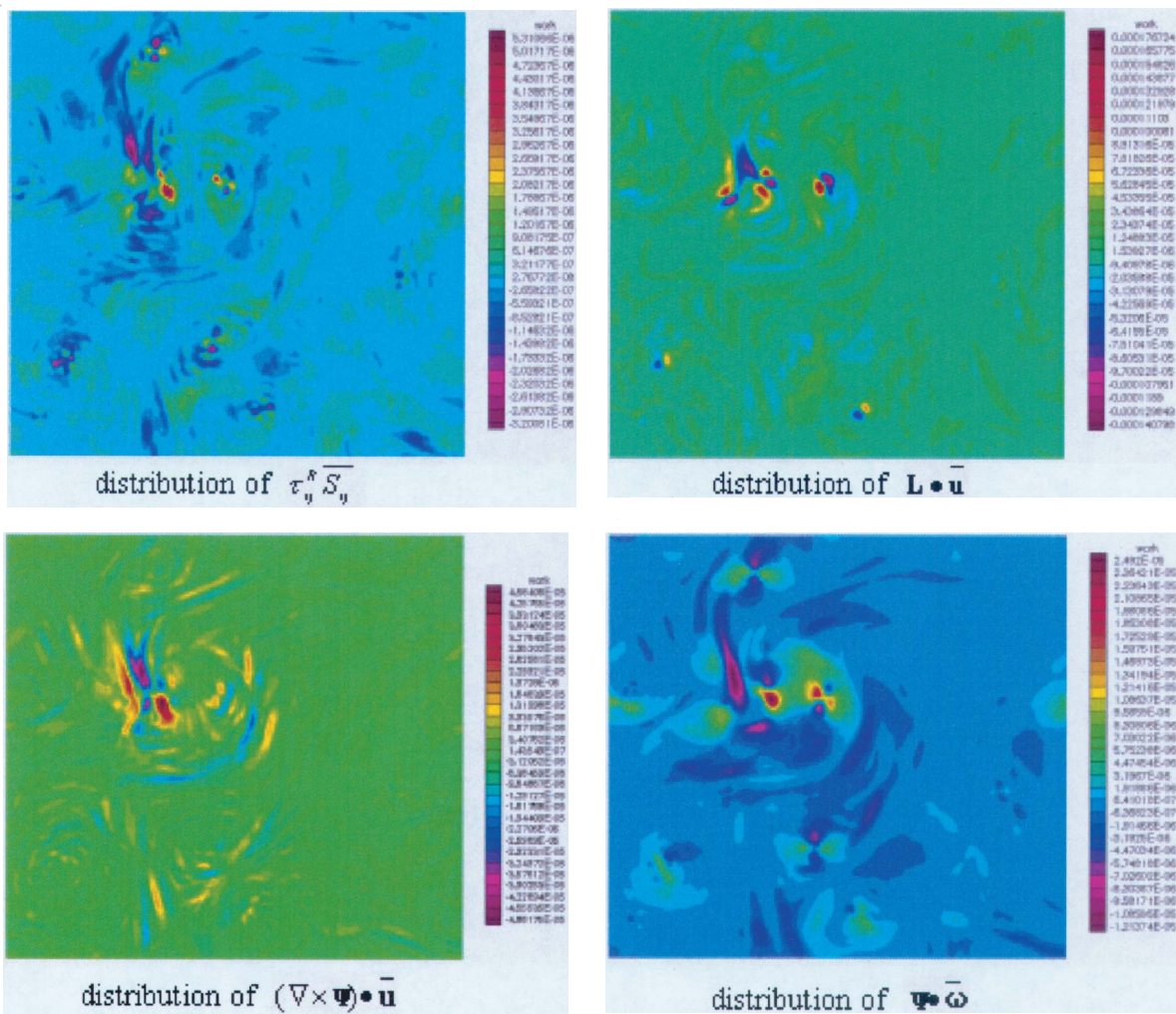


Figure 6. Flood contours of the four forms of energy transfer between resolved scales and subgrid scales.

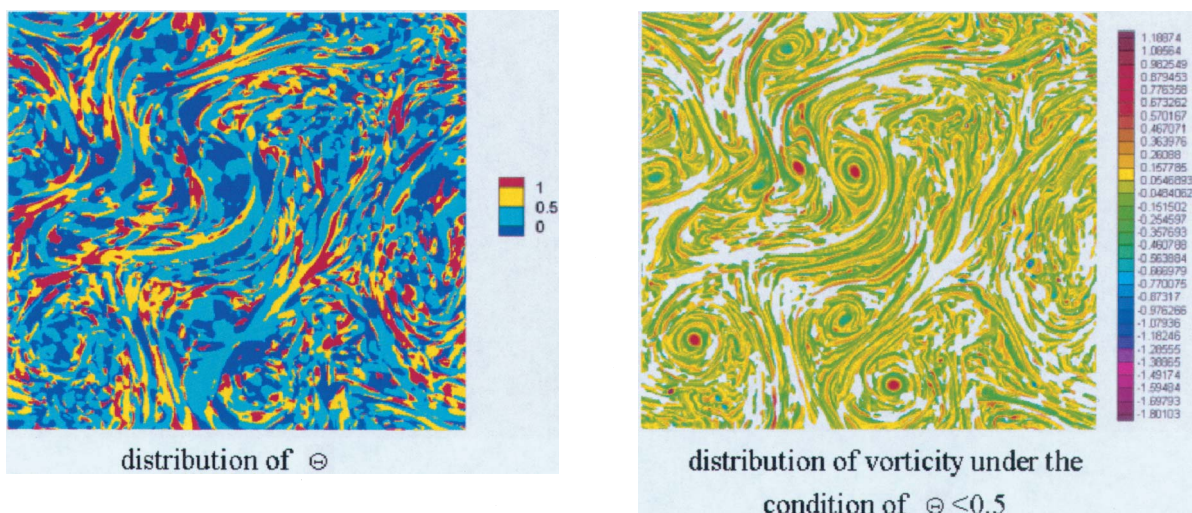


Figure 7. Flood contours of contributive proportion of transverse component over SGS Lamb vector